

Structural properties of phosphatidylcholine in a monolayer at the air/water interface

Neutron reflection study and reexamination of x-ray reflection measurements

David Vaknin,* Kristian Kjaer,* Jens Als-Nielsen,* and Mathias Lösche†

*Physics Department, Risø National Laboratory, DK-4000 Roskilde, Denmark; and †Institute of Physical Chemistry, Johannes-Gutenberg-Universität Mainz, D-6500 Mainz, Germany

ABSTRACT Neutron reflectivities of phosphatidylcholine monolayers in the liquid condensed (LC) phase on ultrapure H₂O and D₂O subphases have been measured on a Langmuir film balance. Using a dedicated liquid surface reflectometer, reflectivities down to $R = 10^{-6}$ in the momentum transfer range $Q_z = 0-0.4 \text{ \AA}^{-1}$ were accessed.

In a new approach, by refining neutron reflectivity data from chain-perdeuterated DPPC-d₆₂ in combination with x-ray measurements on the same monolayer under similar conditions it is shown that the two techniques mutually complement one another. This analysis leads to a detailed conception of the interface structure. It is found that in the LC phase (which is analogous to the L_β phase in vesicle dispersions) the head group is interpenetrated with subphase water (4 ± 2.5 molecules per lipid) and the average tilt angle of the hydrophobic chains from the surface normal is 33 ± 3 degrees.

INTRODUCTION

The microscopic structure of the interface between molecular layers of amphiphilic organic molecules and an aqueous compartment is an important issue in biophysical research as well as in materials science. Floating monolayers on an aqueous subphase present an excellent model system for the investigation of such interfaces and gain increasing importance as an intermediate step for the fabrication of complex functionalized solid-liquid interfaces. The microscopic characterization of such monolayers has received stimulus due to the development of a liquid surface x-ray reflectometer (1) which has been used to determine the structure of, among others, phospholipid monolayers (2-4). We have applied the same principle to construct a liquid surface neutron reflectometer and have measured the reflectivity from interface layers of chain-perdeuterated dipalmitoyl-phosphatidylcholine (DPPC-d₆₂) in the liquid condensed (LC) phase.¹ Although this method cannot match x-ray reflectivity measurements in signal-to-noise ratio and in the reflectivity range accessible (due to the lower beam intensities available as compared to Synchrotron x-ray sources), the option to adjust sample contrast within wide ranges offers undisputable advantages. In fact, as we will show, neutron reflectivity measurements present a means of structure investigation which complements the x-ray method and, in combination with it, can reveal a detailed picture of the interface structure.

Only recently, similar investigations were reported on

comparable systems (6, 7). It was demonstrated that the head group hydration of a monolayer and the ion binding to it can be determined. The work reported here extends further as we quantitatively assess the structure of the interface layer with a careful examination of the confidence one may put in the results. From this investigation we conclude that the information gained from the measurement of either neutron or x-ray reflectivity is limited and only by using results from both types of experiments in a joint model refinement approach we arrive at more definite conclusions.

Closely related in their structure to phospholipid monolayers, aqueous vesicle dispersions have been the subject of numerous studies. During the past decade, detailed microscopic models of these multilayer systems and the intervening water phase were developed (8-11) utilizing x-ray (12-16, 11) and neutron (17, 18, 9) diffraction techniques.

MATERIALS AND METHODS

Neutron reflectometer

Neutron reflectivity measurements were performed on a new liquid surface reflectometer situated in the guide hall of the DR3 reactor at Risø National Laboratory. The reflectometer will be described in detail elsewhere (Vaknin, D., K. Kjaer, and J. Als-Nielsen, manuscript in preparation). It uses a constant wavelength neutron beam (in the range of $\lambda = 3.7-4.8 \text{ \AA}$) which is selected by Bragg reflection from the (002) planes of a Highly Oriented Pyrolytic Graphite crystal (spacing $d = 3.355 \text{ \AA}$, mosaic spread: 0.4° FWHM). The monochromator is mounted on a motorized axis to tilt the normal of the reflecting planes away from the horizontal, consequently bending the incident beam to any desired glancing angle (in the range of $0-7^\circ$) with respect to the liquid surface. The vertical divergence and the vertical angle of

Address correspondence to Dr. M. Lösche.

¹The designation of monolayer phases used is according to reference 5: LC, liquid condensed; LE, liquid expanded.

incidence of the neutron beam onto the sample are controlled by a pair of Gd₂O₃-coated Cd slits of adjustable height and width. The slits are located at the entrance and exit of an 80' Soller collimator which provides horizontal collimation. The incoming neutron intensity is continuously monitored with a ³He (0.05 atm) detector just in front of the sample. Typical intensities of the primary beam at full entrance slit widths ($w = 4$ mm) are $4 \cdot 10^4$ neutrons/s.

The reflected beam is passed through a slit-collimator-slit system in an arrangement symmetrical to the incidence side with a ³He detector (5 atm) in the position symmetrical to the monochromator. A liquid-nitrogen-cooled Be filter mounted between the last slit and the detector discriminates against the $\lambda/2$ component in the beam to better than 2%. For wavelengths in the range of 3.7 Å we found that the $\lambda/2$ component in the primary beam was <6% and need not be filtered. For the determination of the background count rate at each momentum transfer value, Q_z , the detection arm is rotated out of the specular reflection position horizontally to either side by 3°. The reflectometer is controlled by a PC using the software package TASCUM developed at Risø.

Monolayer preparation

Monolayers were prepared in a film balance that has also been used for x-ray reflection experiments and was remodeled to incorporate Al windows to transmit neutron radiation. It contains a glass block within the subphase volume underneath the incident beam footprint area to damp surface waves by reducing the water layer thickness under the film to ~ 300 μm. The film balance is thermostated and the surface pressure π can be determined with a precision of ± 0.1 mN/m.

L- α -perdeutero-dipalmitoyl-phosphatidylcholine (DPPC-d₆₂, purity > 99%; Avanti Polar Lipids, Inc., Birmingham, AL) was used as supplied. Monolayers were spread from a CHCl₃/CH₃OH (3:1) solution (both solvents: p.a.; Merck, Darmstadt, FRG). H₂O for the subphase was purified using a filtration plant (Milli-Q; Millipore Corp., Bedford, MA) and had a conductivity lower than $\sigma = 0.1$ μS · cm. To obtain heavy water subphases of similar quality, D₂O (deuteration purity 99.9 atom%) was distilled five times (four times from KMnO₄) in a quartz/PTFE distillation plant (Normag AG, Hofheim/Ts., FRG). Its conductivity was checked with a hand held conductometer (CG 858; Schott-Geräte, Hofheim/Ts., FRG). With this device we determined values slightly below $\sigma = 1$ μS · cm for both the Millipore-filtered H₂O and the distilled D₂O.² From these checks and, primarily, from the quality of the isotherms (see below), we conclude that the purities of our H₂O and D₂O samples are comparable.

After spreading and solvent evaporation the monolayers were compressed at a speed of 1 Å²/molecule/min to the desired lateral pressure π . Pressure relaxation with DPPC monolayers during data collection was typically <1% per hour. We did, however, recompress the monolayers to the original pressure after taking each data point.

Data collection and data manipulation

As explained above, we evaluate the background (including incoherent scattering from the substrate and general room background) at each individual momentum transfer value, Q_z , thus avoiding a general problem of earlier experiments (6, 7). The background is determined in two measurements with the detection arm of the reflectometer

²We found that some recontamination occurs in the Schott conductometer (lower measurement limit: $\sigma = 0.1$ μS · cm) because our result for H₂O was below $\sigma = 0.1$ μS · cm with the device integrated into the Millipore filtering system.

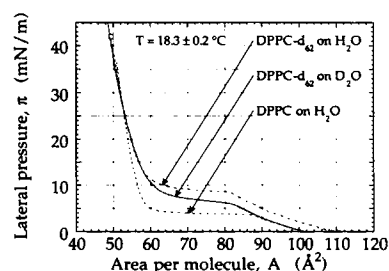


FIGURE 1 Isotherms of hydrogenated or deuterated DPPC on light or heavy pure water subphases, as indicated. Marked on the DPPC-d₆₂/D₂O isotherm is the locus where the neutron and x-ray reflectivities have been measured.

rotated out horizontally to either side of the specular reflection position by 3°. The time interval spent for data collection at each of these two positions was half that for collecting the actual raw reflection datum. The signal was then determined after subtracting the two background values and by normalization to the primary beam intensity and to the efficiency of the primary beam monitor. Finally, the data were divided by the Fresnel reflectivities, R_F , of the respective bare water interfaces and are displayed as R/R_F vs. Q_z because this presentation illustrates the inherent structure of the reflectivity curve more clearly.

Typical count times for each data point (including reflection, background, and monitor signals) was ~ 15 min for momentum transfer values below $Q_z = 0.15$ Å⁻¹ and ~ 45 min above that. Measurement of the whole reflectivity curve then takes 12–14 h. After D₂O experiments, the water was occasionally checked for contamination with H₂O exchanged from the air. In all samples tested the deuteration still amounted to >99 atom%.

RESULTS

Isotope influence on DPPC Isotherms

π vs. A -isotherms of DPPC-d₆₂ measured on top of pure H₂O and D₂O subphases at the same temperature are significantly different. This is demonstrated in Fig. 1, which shows data taken at $T = 18.3 \pm 0.2^\circ\text{C}$: although the general shape is preserved, the monolayer pressure is reduced for the D₂O subphase by about $\Delta\pi = 3$ mN/m over almost the entire range of areas, A .³ It is unlikely that the effect is due to organic contamination of the D₂O because this usually expands a monolayer instead of condensing it. Similarly, we can rule out ionic contamination as the dissolution of, e.g., 10 μM Ca²⁺ (from

³With our measurements of the DPPC-d₆₂ isotherms in the neutron experiment we have not been able to reproduce the A axis to better than 5%. To facilitate a comparison, we have scaled this axis in each data set such that the area per molecule at $\pi = 42$ mN/m is $A = 49$ Å²/molecule (which is the value obtained from reflectivity measurements, see below). Therefore, Fig. 1 should not be misinterpreted as a consistency check for these results.

CaCl₂) into the water subphase acts in condensing a DPPC monolayer by less than $\Delta\pi = 0.2$ mN/m (data not shown). Such a cation concentration, however, would be easily detected due to its conductivity of $\sigma(10 \mu\text{m Ca}^{2+}) \sim 1.2 \mu\text{S} \cdot \text{cm}$. The difference between surface tensions of uncovered H₂O and D₂O is only ~ 0.1 mN/m at 20°C (19), so that we must attribute our observation to an isotope effect specifically affecting the water/phospholipid head group interaction.

The point at $\pi = 42$ mN/m, where the neutron reflectivity data were measured, is marked on the DPPC-d₆₂/D₂O isotherm in Fig. 1. Also included is an isotherm of hydrogenated DPPC on H₂O at $T = 18.2^\circ\text{C}$ which depicts the effect of isotopic substitution of the hydrocarbon chains. This isotherm shows an even larger isotope effect (pressure difference between DPPC-d₆₂ and DPPC monolayers $\Delta\pi = 5.2$ mN/m in the phase transition region) than that of the subphase deuteration. The general structure of phospholipid monolayer isotherms and their temperature dependence have been attributed to an interplay of the internal conformation energy of the hydrocarbon chains and the dispersion interaction between them (20). The elevated transition pressure for DPPC-d₆₂ is then indicative of either a reduced van-der-Waals interaction between the deuterated hydrocarbon chains as compared with hydrogenated ones or of an increase in local disorder, introduced by a higher chain kink density or enhanced vibrational motion, or of both.

Neutron reflectivity from DPPC-d₆₂ monolayers on H₂O and D₂O subphases

We have measured the reflectivity from pure H₂O and D₂O interfaces (Vaknin, D., K. Kjaer, and J. Als-Nielsen, manuscript in preparation) and found good agreement with Fresnel theory for $Q_z < 0.3 \text{ \AA}^{-1}$ (D₂O) and $Q_z < 0.1 \text{ \AA}^{-1}$ (H₂O). The high limits are determined by counting statistics which restrict us to reflectivity values greater than $R = 10^{-6}$. The model calculations included surface roughness. The parameters were determined using a least-squares procedure in the range above 0.015 \AA^{-1} . The results were in quantitative agreement with the literature (scattering length densities of H₂O, $\rho[\text{H}_2\text{O}] = -0.55 \cdot 10^{-6} \text{ \AA}^{-2}$, and of D₂O, $\rho[\text{D}_2\text{O}] = 6.4 \cdot 10^{-6} \text{ \AA}^{-2}$) and earlier x-ray measurements (4) (surface roughness of the interface, $\sigma \sim 3.0 \text{ \AA}$ at $T = 18^\circ\text{C}$).

Reflectivities from DPPC-d₆₂ monolayers were measured at $T = 18^\circ\text{C}$ and $\pi = 42$ mN/m and are displayed in Fig. 2. Shown are the Fresnel-normalized reflectivities, R/R_F , vs. the momentum transfer, Q_z , for H₂O (Fig. 2a) and for D₂O (Fig. 2b) subphases. Included as solid lines

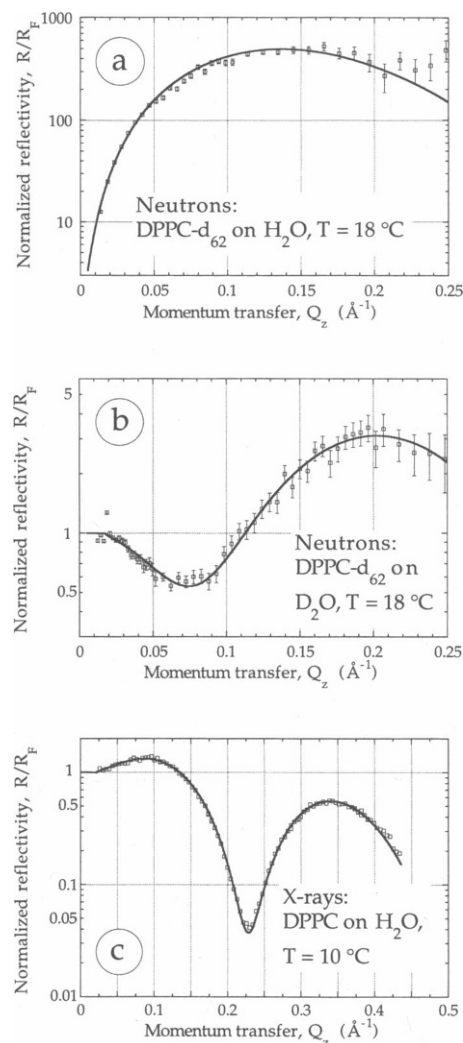


FIGURE 2 Experimental reflectivities of DPPC monolayers in the highly condensed phase with calculated reflectivities (solid lines) from a single model for the three data sets. The data have been normalized to the calculated reflectivities, R_F , of the pure water surfaces.

are the calculated reflectivities based on the best model which is capable of describing both the neutron data and the x-ray data from reference 4 *simultaneously*. In our attempts to develop such a model that reliably describes the microscopic structure normal to the interface we found it imperative to analyze the data sets from x-ray and from neutron experiments in parallel because none of the individual experiments *on its own* leads to a description with reasonable reliability (cf. Fig. 3).

A complication arose due to the fact that the x-ray data sets were taken at temperatures ($T = 10^\circ$ and 23°C) different from that of the neutron experiments. However, by comparing the two x-ray data sets we found that the only model parameter changed beyond the confi-

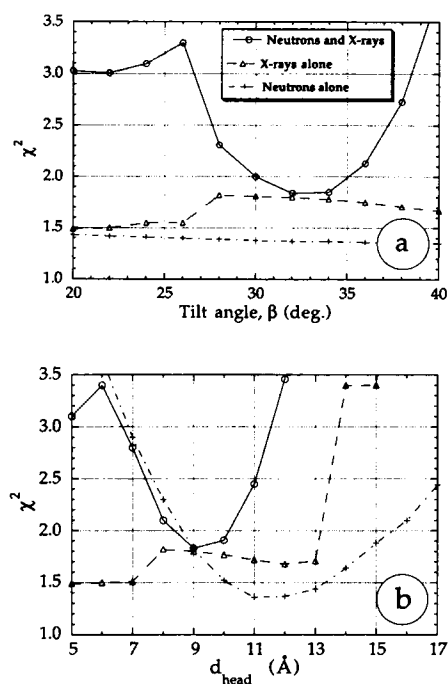


FIGURE 3 Sensitivity of the χ^2 values of best fit modeled reflectivities describing the experimental data to fixed values of one of the adjustable parameters. (a) Chain tilt angle, β , varied in discrete steps while all other independent parameters adjusted; (b) head group layer thickness, d_{head} , varied in discrete steps while all other independent parameters adjusted.

dence limits of the fits is the surface roughness σ . Consequently, we included four different results, two from x-ray and two from neutron reflectivity measurements, into a global data set and allowed only the surface roughness to vary individually within each subset when determining the best universal model. We feel this is a reasonable simplification given the fact that the monolayer does not change its phase state at constant pressure within this temperature interval. Fig. 2 c shows the experimental x-ray data set at $T = 10^\circ\text{C}$ (4) with the modeled reflectivity as a solid line.

We adopted a two-box model (with two constant scattering length density regions, cf. references 4, 7, and 9) to calculate reflectivities using the Parratt recursion formalism (21). The scattering length densities used were obtained from standard values of the scattering lengths and the geometric parameters of the model.⁴

⁴Note added in proof: This approach is analogous to the simultaneous modeling procedure of x-ray and neutron diffraction data in the structure determination of phosphatidylcholine multibilayer systems developed by Wiener and White which they call *Composition-Space Refinement* (37).

The independent parameters whose values were obtained from the fitting procedure were (a) the cross-section, A_0 , of a lipid molecule normal to the direction of the extended hydrocarbon chains; (b) the tilt angle, β , of the chains (assumed close packed) from the surface normal; (c) the thickness, d_{head} , of the lipid head group layer projected on the surface normal; and (d) the number, N_w , of the water molecules interpenetrating the lipid head group. All other geometric quantities were either assumed to be known (such as the length of the extended palmitoyl chain, $l_{\text{chain}} = 19.15 \text{ \AA}$, references 22 and 2, or the volume of a water molecule, $V_w = 30 \text{ \AA}^3$) or were dependent (such as the area per lipid molecule parallel to the surface, $A = A_0/\cos \beta$, the thickness of the box describing the lipid chain region, $d_{\text{chain}} = l_{\text{chain}} \cdot \cos \beta$, or the volume of the water-free lipid head group, $V_{\text{head}} = A \cdot d_{\text{head}} - N_w \cdot V_w$). This procedure differs from earlier approaches to data evaluation (4) in that then an *assumption*, $A = 46 \text{ \AA}^2$, was made in accordance with published isotherms (23) to reduce the parameter space and the independent parameters were confined within specific ranges.

To substantiate our statement that neither of the two techniques *by itself* is capable of modeling the interface structure, Fig. 3 shows the minimal χ^2 values for different fixed values of one parameter (the chain tilt angle, β , in Fig. 3 a or the head group layer thickness, d_{head} , in Fig. 3 b) and all other independent parameters adjusted. The absolute value of χ^2 was calculated using

$$\chi^2(\mathbf{a}) = \frac{1}{N - P} \sum_{i=1}^N \left(\frac{R_i - R(Q_i, \mathbf{a})}{\sigma_i} \right)^2,$$

where \mathbf{a} is the P -dimensional parameter set defining the model R , $R_i \pm \sigma_i$ denote the experimental reflectivity data and standard deviations at momentum transfer values Q_i , and N is the number of data points. Models were fitted to the neutron and the x-ray data sets *alone* and to the combined data set as indicated in the figure. For the combined data set, $N = 263$ and $P = 6$ (three out of four structural parameters varied, see Table 1, plus three differing surface roughness values, see Table 2). Clearly this presentation demonstrates how the two techniques complement one another.

Table 1 is a compilation of determined best fit values for the adjusted parameters and calculated results for the dependent variables of the model. Our criterion for the quantification of the confidence limits was a 15% increase of χ^2 from its minimal value when changing the respective parameter while readjusting all the others to a new local minimum. It may seem odd at a first glance to include both $A_0 = A \cdot \cos \beta$ and β as independent parameters into the fitting procedure because A can in principle be determined independently from the iso-

TABLE 1 DPPC monolayer structure on the surface of pure water at $\pi = 42$ mN/m

A_0	$41.2 \pm 0.5 \text{ \AA}^2$	(Cross-section of a lipid molecule in film)
β	$33 \pm 3^\circ$	(Chain tilt angle from surface normal)
d_{head}	$9.3 \pm 1 \text{ \AA}$	(Thickness of lipid head group layer)
N_w	4 ± 2.5	(Number of water molecules in head group)
$A (= A_0/\cos\beta)$	$49.1 \pm 2 \text{ \AA}^2$	(Area per lipid molecule in surface film)
$d_{\text{chain}} (= l_{\text{chain}} \cdot \cos\beta)$	$16.0 \pm 0.6 \text{ \AA}$	(Thickness of lipid chain group layer)
$d_{\text{total}} (= d_{\text{head}} + d_{\text{chain}})$	$25.3 \pm 0.4 \text{ \AA}$	(Total interface film thickness)
$V_{\text{head}} (= A \cdot d_{\text{head}} \cdot N_w \cdot V_w)$	$335 \pm 8 \text{ \AA}^3$	(Volume of the "dry" lipid head group)
$V_{\text{total}} (= V_{\text{head}} + A \cdot d_{\text{chain}})$	$1124 \pm 4 \text{ \AA}^3$	(Volume of lipid molecule in film)
(constants: $l_{\text{chain}} = 19.15 \text{ \AA}$; $V_w = 30 \text{ \AA}^3$)		

Best fit parameters (*upper part*) from a fit to four experimental data sets (two neutron reflectivity and two x-ray reflectivity) as described in the text, and calculated dependent parameters (*lower part*).

therms. However, in our attempts to model the interface structure we found A consistently larger than in the literature (23) and consequently decided to determine it independently to arrive at a self-consistent picture.

Similar to the situation reported from structural investigations of vesicle dispersions (11) we find that some results are determined with poor accuracy ($N_w = 4 \pm 60\%$; $d_{\text{head}} = 9.3 \text{ \AA} \pm 10\%$) and some with higher accuracy ($V_{\text{head}} = 335 \pm 3\%$). The reason for this is the strong correlation between some parameters while others are virtually independent. For instance, the dimension, $d = d_{\text{chain}} + 1/2 \cdot d_{\text{head}}$ evaluates to $d = 20.65 \pm 0.1 \text{ \AA}$, and is extremely sensitive to the sharp dip in the x-ray reflectivity around $Q_z^{\text{min}} = 0.228 \text{ \AA}^{-1}$ ($d \cong 3\pi/2/Q_z^{\text{min}}$, references 2 and 24). It has to be stressed, however, that the error limits given represent the statistical uncertainties and do not include an estimate of systematic deviations, possibly caused by the difference in temperatures of the x-ray and neutron data sets. The calculated parameters of the two-box models that lead to the modeled reflectivities presented in Fig. 2 are listed in Table 2.

We have also tried a three-box model as an alternative description of the interface, parsing the lipid head group in two portions that contain the glycerol backbone and

the choline moiety, respectively. The result obtained from the best fit is in general consistent with the two-box model. It indicates that more water molecules are associated with the glycerol than with the choline part. However, the χ^2 minimum in the parameter space is so flat that we have to regard this result as a hint rather than a definite conclusion.

DISCUSSION

In this work we aim at the refinement of the structural information obtained from earlier x-ray investigations and argue that a valid model for an organic monolayer at the liquid interface has to be consistent with the results from *both* techniques, x-ray as well as neutron reflectivities. The obvious advantage of the neutron reflection method is the possibility of varying the scattering length densities of both the interface film and the liquid subphase over wide ranges by means of isotope substitution. Hence, it is possible to concentrate on particular regions of the molecules at the surface. An inherent assumption of this approach is that intermolecular and intramolecular interactions are not affected by the substitution. This assumption is certainly a sound one to

TABLE 2 Surface roughness and scattering length densities of the two-box model of a DPPC monolayer on a water subphase at $\pi = 42$ mN/m

	Neutrons DPPC-d ₅₂ , $T = 18^\circ\text{C}$		X-Rays DPPC on H ₂ O	
	on D ₂ O	on H ₂ O	$T = 10^\circ\text{C}$	$T = 23^\circ\text{C}$
σ	$3.6 \pm 0.5 \text{ \AA}$	$3.6 \pm 0.5 \text{ \AA}$	$3.6 \pm 0.1 \text{ \AA}$	$4.2 \pm 0.1 \text{ \AA}$
ρ_{chain}	$7.8 \pm 0.1 \cdot 10^{-6} \text{ \AA}^{-2}$		$0.307 \pm 0.003 \text{ e/\AA}^3$	
ρ_{head}	$3.0 \pm 0.6 \cdot 10^{-6} \text{ \AA}^{-2}$	$1.2 \pm 0.3 \cdot 10^{-6} \text{ \AA}^{-2}$	$0.447 \pm 0.013 \text{ e/\AA}^3$	
ρ_{water}	$6.39 \cdot 10^{-6} \text{ \AA}^{-2}$	$-0.56 \cdot 10^{-6} \text{ \AA}^{-2}$	0.334 e/\AA^3	

The scattering length densities were calculated from the best-fit parameters given in Table 1 and used to compute the reflectivities included in Fig. 2 as solid lines.

a first approximation as the isotope substitution has no influence on the chemical identity of a molecular species. However, it *does* affect the weaker interactions between molecules or atom groups within molecules, and with hydrogen/deuterium substitution differences are most pronounced.

As seen from the isotherms (cf. Fig. 1), the perdeuteration of the phospholipid tails affects the interaction quantitatively, although not qualitatively. A similar effect was observed by D. Allan Cadenhead (an elevation of the phase coexistence pressure of DPPC-d₆₂ from the DPPC value of $\Delta\pi \sim 8$ mN/m on a 100 mM NaCl subphase at pH = 5.5, unpublished personal communication). In a volumetric study the main phase transition temperature of DMPC vesicles was found $\Delta T_m = 5.1^\circ\text{C}$ above that of DMPC-d₅₄ (25). This reflects a behavior identical to our observation both qualitatively (i.e., it indicates a reduction of the dispersion interaction or an increase of conformational disorder on deuteration) and quantitatively (with the estimate that a pressure difference of $\Delta\pi = 5$ mN/m can be compensated for by a temperature difference of $\Delta T = -5^\circ\text{C}$ in DPPC monolayers, see reference 23).

Turning to the subphase, the physical properties of H₂O and D₂O are rather comparable, and the surface tension values at room temperature agree within 0.2% (19). Therefore it was a surprise to find a marked dependence of the interactions between the liquid substrate and the phospholipid monolayer on the isotope (H₂O/D₂O) content. A comparison of stearic acid monolayers on H₂O and D₂O (26) found identical isotherms in both situations in the condensed states whereas a pressure reduction on the D₂O subphase was reported at low pressures, qualitatively similar to our observation. The surface normal projected dipole moment per lipid molecule at the interface was reported to be increased by $\sim 5\%$ on the D₂O subphase (26). As in the case of the chain deuteration, vesicle dispersions show water deuteration-dependent shifts in their phase transition temperatures (27, 28) that are qualitatively consistent with our findings although this effect is about five times larger with the monolayer experiments. At present we can only speculate on an increased strength of deuterium bonds compared with hydrogen bonds to the polar parts of the phospholipid head groups. We are not aware of any discussion of the observed effect in the literature with the exception of one case (29) where a similar observation was reported from a comparable, albeit rather ill-defined, system. It appears to us, however, that our observation unravels the possibility for specifically investigating the water/phospholipid head group interaction and calls for more efforts from both the experimental and theoretical side.

Refined structure model of DPPC monolayers at high lateral pressure

We have chosen to concentrate this study on the highly condensed LC state at $\pi = 42$ mN/m because here the monolayer is in the same state independent of its composition in terms of the isotopes incorporated (see Fig. 1) and, moreover, corresponding data are available from x-ray measurements (4). From the results tabulated in Table 1 the following conclusions can be drawn:

(a) The lipid molecules within the surface monolayer are in a near to close-packed arrangement. This conclusion is reached from a comparison of the value of $A_0 = 41.2 \text{ \AA}^2$ to the cross-section area of two crystalline acyl chains in a monolayer ($2 \cdot 19.8 \text{ \AA}^2$; reference 30), or to the corresponding values from hydrated DPPC vesicle dispersions in the L_c ($2 \cdot 20.0 \text{ \AA}^2$; reference 10) or in the L_{β'} ($2 \cdot 20.3 \text{ \AA}^2$; reference 10) phases. Furthermore, we find the (dry) volume of a lipid molecule in the film, $V_{\text{lipid}} = V_{\text{head}} + A \cdot d_{\text{chain}} = 1,124 \pm 4 \text{ \AA}^3$, very close to corresponding results from vesicle dispersions ($V_{\text{lipid}} = 1,140 \pm 10 \text{ \AA}^3$; reference 25 and $V_{\text{lipid}} = 1,144 \pm 2 \text{ \AA}^3$; reference 11). Obviously, our result is what would be expected at such a high monolayer pressure, but the fact that it is obtained without any additional assumption demonstrates how first-hand information can be extracted from the reflectivity measurements. Finally, it is worthwhile mentioning that we have obtained the area per lipid molecule at $\pi = 42$ mN/m, $A = 49.1 \pm 2 \text{ \AA}^2$, *independently* from the isotherm. This area has been taken to be $A = 46 \text{ \AA}^2$ in the former x-ray work (4).

(b) The large value of the chain tilt angle β reflects the large mismatch between the cross-section of the choline head group and the acyl chains of the DPPC molecule. This result, again, is obtained without additional assumptions. Once more, our result matches the structure found in the L_{β'} phase of hydrated DPPC vesicle dispersions, $\beta = 30 \pm 3^\circ$ (11).

(c) Our results pertaining to the head group part of the lipid molecule agree perfectly with the L_{β'} phase vesicle results as far as its volume, V_{head} , is concerned (11). Major differences only arise with respect to the hydration number, N_w , and layer thickness, d_{head} . This is not too surprising given the fact that the monolayer lipid/water interface lacks the close by counter interface present in multilamellar stacks. We find significantly larger values of both N_w and d_{head} which is a strong indication that unlike the stacked multibilayers (17) the head group is *not* oriented with its dipole direction parallel to the surface but protrudes more deeply into the water subphase. On the other side, from DSC experiments on DPPC dispersions it was concluded that the lipid head group contains five firmly bound water molecules in the L_{β'} phase (31). Independent support for

our result of a large penetration depth of the head group into the water subphase comes from studies of antibody binding to haptens anchored within DPPC monolayers (32). A systematic variation of the spacer length, l , between the surface and the epitope that binds to the antibody showed that no specific binding occurs for $l = 6$ Å. At $l = 10$ Å, binding was observed to a monolayer in the expanded state, LE. Still, on compression of the monolayer the protein was detached at lateral pressures, $\pi > 20$ mN/m, which was attributed to steric hindrance between the antibody and the choline group.

CONCLUSIONS

Combined neutron and x-ray reflectivity measurements provide a sensitive means for the structure investigation of floating monolayers at liquid interfaces. We have demonstrated that a detailed conception of the interface structure can be obtained in a selfconsistent way. We have in particular worked out the chain-packing characteristics and have quantified the head group layer thickness and water interpenetration into the lipid head group for a single point in the phase diagram of DPPC monolayers. Most of our findings are in quantitative agreement with results from structure investigations of DPPC in aqueous dispersions. Here, major discrepancies are encountered only for the details of the head group arrangement and for its hydration. These discrepancies are attributed to the marked difference between the two model systems that in the multibilayer case there are closely opposing counter surfaces which the monolayer lacks.

We have refrained from comparing our results with earlier findings from neutron reflection measurements on mixed DMPC/DMPG monolayers (7), as the information on the modeling of data provided there is rather scarce. This contrasts with the very detailed conclusions reached in their interpretation. In view of our results shown in Fig. 3 we suggest that the conclusions drawn in reference 7 may be somehow speculative. Similarly, we argue that results from x-ray reflectivity measurements should be interpreted very carefully and models inferred from them need to be constructed in a selfconsistent way.

We have not undertaken this investigation of interface monolayers to supply structural arguments for a comparison of such model systems with lipid vesicles or cell membranes. The relationship between these systems has been extensively discussed in the literature (20, 25, 33–36) and one of the most disputed questions, at which values of the thermodynamic variables the states of lipid molecules in a monolayer or in a bilayer correspond to each other, cannot be resolved because the answer

depends on *which* variable one is using as a criterion. As we have shown, we find a close structural relation between both systems at a monolayer pressure, $\pi = 42$ mN/m. However, we also have clear indications that the head group structure may differ significantly. Our main interest in undertaking this effort was to characterize the interface for its further utilization as a target for the study of specific recognition processes between ligand/receptor systems, an investigation which is currently in progress (Vaknin, D., J. Als-Nielsen, M. Piepenstock, and M. Lösche, manuscript in preparation).

We thank K. Theodor and J. Linderholm for technical assistance, the Chemistry Department of Risø National Laboratory for the supply of highly purified H₂O, G. Decher for invaluable advice in designing the D₂O distillation plant, J. Skov Pedersen for valuable suggestions on the model refinement, and P. A. Lindgård, G. Brezesinski, D. A. Cadenhead, W. Knoll, and H. Möhwald for helpful discussions.

It is our pleasure to acknowledge joint financial support for the construction of the neutron reflectometer from the NOVO foundation, the Carlsberg foundation, and the Danish Science Research Council as well as financial support from the German Bundesministerium f. Forschung und Technologie under contract no. 05 453 FA 19.

Received for publication 17 December 1990 and in final form 15 February 1991.

REFERENCES

1. Als-Nielsen, J., and P. S. Pershan. 1983. Synchrotron x-ray radiation study of liquid surfaces. *Nucl. Instrum. Methods.* 208:545–548.
2. Als-Nielsen, J., and K. Kjaer. 1989. X-ray reflectivity and diffraction studies of liquid surfaces and surfactant monolayers. In *Phase Transitions in Soft Condensed Matter*. T. Riste and D. Sherrington, editors. Plenum Press, New York. 113–138.
3. Als-Nielsen, J., and H. Möhwald. 1991. Synchrotron x-ray scattering studies of Langmuir films. In *Handbook of Synchrotron Radiation*. S. Ebashi, E. Rubenstein, and M. Koch, editors. Elsevier/North Holland, Amsterdam. In press.
4. Helm, C. A., H. Möhwald, K. Kjaer, and J. Als-Nielsen. 1987. Phospholipid monolayer density distribution perpendicular to the water surface. A synchrotron x-ray reflectivity study. *Europhys. Lett.* 4:697–703.
5. Cadenhead, D. A., F. Müller-Landau, and B. M. J. Kellner. 1980. Phase transitions in insoluble one and two-component films at the air/water interface. In *Ordering in Two Dimensions*. S. K. Sinha, editor. Elsevier/North Holland, Amsterdam. 73–81.
6. Grundy, M. J., R. M. Richardson, S. J. Roser, J. Penfold, and R. C. Ward. 1988. X-ray and neutron reflectivity from spread monolayers. *Thin Solid Films.* 159:43–52.
7. Bayerl, T. M., R. K. Thomas, J. Penfold, A. Rennie, and E. Sackmann. 1990. Specular reflection of neutrons at phospholipid monolayers. Changes of monolayer structure and head-group hydration at the transition from the expanded to the condensed phase state. *Biophys. J.* 57:1095–1098.

8. Ruocco, M. J., and G. G. Shipley. 1982. Characterization of the sub-transition of hydrated dipalmitoylphosphatidylcholine bilayers. X-ray diffraction study. *Biochim. Biophys. Acta*. 684:59–66.
9. King, G. I., and S. H. White. 1986. Determining bilayer hydrocarbon thickness from neutron diffraction measurements using strip-function models. *Biophys. J.* 49:1047–1054.
10. Nagle, J. F., and M. C. Wiener. 1989. Relations for lipid bilayers. Connection of electron density profiles to other structural quantities. *Biophys. J.* 55:309–313.
11. Wiener, M. C., R. M. Suter, and J. F. Nagle. 1989. Structure of the fully hydrated gel phase of dipalmitoylphosphatidylcholine. *Biophys. J.* 55:315–325.
12. Parsegian, V. A., N. Fuller, and R. P. Rand. 1979. Measured work of deformation and repulsion of lecithin bilayers. *Proc. Natl. Acad. Sci. USA*. 76:2750–2754.
13. Lis, L. J., M. McAlister, N. Fuller, R. P. Rand, and V. A. Parsegian. 1982. Interaction between neutral phospholipid bilayer membranes. *Biophys. J.* 37:657–666.
14. Ruocco, M. J., and G. G. Shipley. 1982. Characterization of the sub-transition of hydrated dipalmitoylphosphatidylcholine bilayers. Kinetic, hydration and structural study. *Biochim. Biophys. Acta*. 691:309–320.
15. McIntosh, T. J., and S. A. Simon. 1986. Area per molecule and distribution of water in fully hydrated dilauroylphosphatidylethanolamine bilayers. *Biochemistry*. 25:4948–4952.
16. McIntosh, T. J., A. D. Magid, and S. A. Simon. 1989. Range of the solvation pressure between lipid membranes: dependence on the packing density of solvent molecules. *Biochemistry*. 28:7904–7912.
17. Büldt, G., H. U. Gally, J. Seelig, and G. Zaccari. 1979. Neutron diffraction studies on phosphatidylcholine model membranes. I. Head group formation. *J. Mol. Biol.* 134:673–691.
18. Zaccari, G., G. Büldt, A. Seelig, and J. Seelig. 1979. Neutron diffraction studies on phosphatidylcholine model membranes. II. Chain conformation and segmental order. *J. Mol. Biol.* 134:693–706.
19. Landolt-Börnstein. Zahlenwerte und Funktionen aus Physik, Chemie, Astronomie, Geophysik und Technik. 1964. 6th ed. K. Schäfer and E. Lax, editors. Springer, Berlin. II, 3:421–422.
20. Marčelja, S. 1974. Chain ordering in liquid crystals. II. Structure of bilayer membranes. *Biochim. Biophys. Acta*. 367:165–176.
21. Parratt, L. G. 1954. Surface studies of solids by total reflection of x-rays. *Phys. Rev.* 95:359–369.
22. Tanford, C. 1972. Micelle shape and size. *J. Phys. Chem.* 76:3020–3024.
23. Albrecht, O., H. Gruler, and E. Sackmann. 1978. Polymorphism of phospholipid monolayers. *J. Phys. (Paris)*. 39:301–313.
24. Kjaer, K., J. Als-Nielsen, C. A. Helm, P. Tippmann-Krayer, and H. Möhwald. 1988. An x-ray scattering study of lipid monolayers at the air-water interface and on solid supports. *Thin Solid Films*. 159:17–28.
25. Schmidt, G., and W. Knoll. 1985. Densitometric characterization of aqueous lipid dispersions. *Ber. Bunsenges. Phys. Chem.* 89:36–43.
26. Dreher, K. D., and D. F. Sears. 1966. Stearic acid monolayers on heavy water. *Trans. Faraday Soc.* 62:741–749.
27. Lipka, G., B. Z. Chowdhry, and J. M. Sturtevant. 1984. A comparison of the phase transition properties of 1,2-diacylphosphatidylcholines and 1,2-diacyl-phosphatidylethanolamines in H₂O and D₂O. *J. Phys. Chem.* 88:5401–5406.
28. Wiener, M. C., S. Tristram-Nagle, D. A. Wilkinson, L. E. Campbell, and J. F. Nagle. 1988. Specific volumes of lipids in fully hydrated bilayer dispersions. *Biochim. Biophys. Acta*. 938:135–142.
29. Kremlev, I. N., and V. I. Lobyshev. 1985. Compressibility of phospholipid monolayers in different phasic state in H₂O and D₂O. *Biophysics*. 30:74–78. (*Biophysika*. 30:72–75 [in Russian].)
30. Kjaer, K., J. Als-Nielsen, C. A. Helm, P. Tippmann-Krayer, and H. Möhwald. 1989. Synchrotron x-ray diffraction and reflection studies of arachidic acid monolayers at the air-water interface. *J. Phys. Chem.* 93:3200–3206.
31. Dörfler, H., and G. Brezesinski. 1983. Phasenumwandlungerscheinungen in Lecithin/Wasser-Systemen I. Einfluß des Wassers auf die Phasenumwandlungen homologer Lecithin/Wasser-Monohydrate. *Colloid & Polym. Sci.* 261:286–292 (in German).
32. Piepenstock, M., M. Lösche, and H. Möhwald. Local control of antibody binding to hapten-presenting interfaces: steric and electrostatic interactions. In *Die Makromolekulare Chemie. Proc. 3rd Europ. Conf. Organic Thin Films*. Peterson, I. R., editor. In press.
33. Oldani, D., H. Hauser, B. W. Nichols, and M. C. Phillips. 1975. Monolayer characteristics of some glycolipids at the air-water interface. *Biochim. Biophys. Acta*. 382:1–9.
34. Hui, S. W., M. Cowden, D. Papahadjopoulos, and D. F. Parsons. 1975. Electron diffraction study of hydrated phospholipid single bilayers. Effects of temperature, hydration and surface pressure of the "precursor" monolayer. *Biochim. Biophys. Acta*. 382:265–275.
35. Blume, A. A comparative study of the phase transitions of phospholipid bilayers and monolayers. *Biochim. Biophys. Acta*. 557:32–44.
36. Nagle, J. F. 1980. Theory of the main lipid bilayer phase transition. *Annu. Rev. Phys. Chem.* 31:157–195.
37. Wiener, M. C., and S. H. White. 1991. Fluid bilayer structure determination by the combined use of x-ray and neutron diffraction. II. "Composition-space refinement" method. *Biophys. J.* 59:174–185.